Antarctic permafrost degassing in Taylor Valley by extensive soil gas investigation

Ruggiero L.[a], Sciarra A.[a*], Mazzini A.[b,a], Florindo F.[a], Wilson G.[c,d], Tartarello M.C.[e], Mazzoli C.[f], Anderson J.T.H.[d], Romano V.[e], Worthington R.[d], Bigi S.[e], Sassi R.[f] and Ciotoli G.[g,a]

[a] Istituto Nazionale di Geofisica e Vulcanologia, Sezione di Roma, Via Vigna Murata 605, 00143 Roma, Italy
[b] Center of Earth Evolution and Dynamics, University of Oslo, Sem Sælandsvei 2A, 0371 Oslo, Norway
[c] GNS Science, PO Box 30-368, Lower Hutt 5040, New Zealand
[d] Department of Marine Science, University of Otago, PO Box 56, Dunedin 9054, New Zealand
[e] Earth Science Department, "Sapienza" University of Rome, Piazzale Aldo Moro 5, 00185 Roma, Italy
[f] Department of Geosciences, University of Padua, Via Gradenigo 6, 35131 Padova, Italy
[g] National Research Council, Institute of Environmental Geology and Geoengineering, CNR-IGAG, Area della Ricerca di Roma 1- Strada Provinciale 35d, 9 – 00010, Montelibretti (Rome), Italy

*Corresponding Author
alessandra.sciarra@ingv.it

Abstract

Ongoing studies conducted in northern polar regions reveal that permafrost stability plays a key role in the modern carbon cycle as it potentially stores considerable quantities of greenhouse gases. Rapid and recent warming of the Arctic permafrost is resulting in significant greenhouse gas emissions, both from physical and microbial processes. The potential impact of greenhouse gas release from the Antarctic region has not, to date, been investigated. In Antarctica, the McMurdo Dry Valleys comprise 10% of the ice-free soil surface areas in Antarctica and like the northern polar regions are also warming albeit at a slower rate.

The work presented herein examines a comprehensive sample suite of soil gas (e.g., CO_2, CH_4 and He) concentrations and CO_2 flux measurements conducted in Taylor Valley during austral summer 2019/2020. Analytical results reveal the presence of significant concentrations of CO_2, CH_4 and He (up to 3.44 vol%, 18,447 ppmv and 6.49 ppmv, respectively) at the base of the active layer. When compared with the few previously obtained measurements, we observe increased CO_2 flux rates (estimated CO_2 emissions in the study area of 21.6 km^2 ≈ 15 tons day^{-1}). We suggest that the gas source is connected with the deep brines migrating from inland (potentially from beneath the

Antarctic Ice Sheet) towards the coast beneath the permafrost layer. These data provide a baseline for future investigations aimed at monitoring the changing rate of greenhouse gas emissions from Antarctic permafrost, and the potential origin of gases, as the southern polar region warms.

Highlights:

- First extensive soil gas and flux survey in Antarctica.
- Discovered zones of multigas (CO_2, CH_4, He, H_2) anomalies.
- CO_2 emissions estimation in Lower Taylor Valley.
- Gas rising from deep brines

Key words: Permafrost, soil gas survey, CO_2 output, McMurdo Dry Valleys, Antarctica

1 Introduction

Permafrost is defined as any ground (soil or rock and any ice and organic material inclusions) that remains completely frozen (0 °C or colder) for at least two years (Van Everdingen, 2005). It is present in both hemispheres at high latitudes and its temperature, thickness, and continuity are controlled by the geographic setting and, to a large extent, by the surface energy balance (Schuur et al., 2008). Climate warming effects are going to impact these regions in the upcoming decades (Shindell et al., 2004; Chapman et al., 2007) and all three types of permafrost (dry, ice-cemented, and massive ice) present below 1000 m elevation may be susceptible to warming-related degradation depending on future emission pathways (Hagedorn et al., 2007; Swanger & Marchant, 2007). Permafrost thawing and the microbial decomposition of previously frozen organic carbon is considered one of the most likely positive climate feedbacks from terrestrial ecosystems to the atmosphere (Schuur et al., 2015; Xue et al., 2016). Measurements of CO_2 and CH_4 soil concentrations and fluxes are essential to understand the C cycle in terrestrial ecosystems, although less is known about controls over CO_2 flux (φCO_2) in ecosystems lacking vascular vegetation, including polar deserts and some hot deserts,

where autotrophic inputs are low and abiotic factors tend to dominate in determining φCO_2 (Shanhun et al., 2012).

In the Arctic and boreal regions, permafrost is found in Greenland, Alaska, Canada, Northern Europe, Russia, and China (Schuur et al., 2008), and represents about 17% of the exposed land surface (Gruber, 2012). Studies carried out on permafrost soils in these ecosystems have shown these areas store almost twice the carbon currently present in the atmosphere (Schuur et al., 2008, 2009). These regions are rich in frozen organic matter, that would lead to an increase of the production of CO_2 and CH_4 by microbial activities in case of thawing (Schuur et al., 2008). Furthermore, part of the released carbon could easily dissolve in water and, through solar radiation, produce CO_2 by the photo mineralization process (Cory et al., 2014). Large methane deposits currently stored at high latitude regions are either frozen within permafrost or trapped below impermeable buffer zones (Anthony et al, 2012). Methane has a global warming potential 28 times higher than that of CO_2 on a 100-year time horizon (Ciais et al, 2013). It is therefore imperative to provide estimates of methane and other gases released from the high-latitude regions. In remote and scarcely monitored regions soil gas release can endure for decades or even centuries before being detected and quantified.

In the Southern Hemisphere, permafrost soils are found at high elevations, in the Sub-Antarctic islands, in the Antarctic Peninsula and in the ice-free areas of the Antarctic region. Permafrost degradation in the Antarctic continent has not been widely studied (Levy et al., 2013) due to terrain limitations (i.e., ice-free area represents only 0.35% of the continent; Campbell & Claridge, 2009) and the overall limited organic content in soils (Schuur et al., 2008) making it less relevant for atmospheric carbon contributions. However, the role of microbial activity in Antarctic soils could potentially be more important than previously believed. Indeed, microbial activity affects the amount of total organic carbon and is more susceptible to weak temperature variations (Schuur et al., 2008). The McMurdo Dry Valleys (thereafter MDV) are the largest ice-free regions in Antarctica (Gilichinsky et al., 2007); and their geomorphology reveals how the landscape is strongly controlled

by climate processes (Fountain et al., 2014). Attempts to quantify CO_2 emissions on the Antarctic continent have been carried out in the MDV soils, highlighting that φCO_2 is driven primarily by physical factors such as soil temperature and moisture, indicating that future climate change may alter the soil C cycle (Elberling et al., 2006; Bockheim et al., 2007; Gilichinsky et al., 2007; Ball et al., 2009; MacIntyre et al., 2019). The lack of mechanistic understanding makes it difficult to predict the contribution of soil φCO_2 to the C-cycle due to climate change in the polar deserts of Antarctica. In the MDV, φCO_2 has been used to characterize a variety of ecosystem processes and properties, including soil C turnover, the functional role of differing origins of organic matter supporting C cycling, and biotic distribution and activity (Virginia et al., 1999; Burkins et al., 2001; Adams et al., 2006; Barrett et al., 2006; Hopkins et al., 2006).

To date, φCO_2 studies conducted in MDV soils were performed on few measurement points. Results revealed low values that are highly uncertain and spatially variable (Gregorich et al., 2006; Burke et al., 2017). It is therefore difficult to separate the biological processes (e.g., C-fixation, heterotrophic respiration) from physical factors (e.g., carbonate dissolution). Parsons et al. (2004) suggested that in extreme desert environments, abiotic factors, like temperature gradients, parent material and soil water dynamics, may have the same magnitude of the biological processes influencing φCO_2 rates; on the contrary, in mid-latitude ecosystems the physical φCO_2 is often negligible.

Recent studies have revealed a diffuse subsurface brine system in the MDV area. This occurs preferentially near the coast and under the surface sediments of the main valleys and is sourced beneath the East Antarctic Ice Sheet (Mikucki et al., 2015). The presence of this deep fluid circulation may also favour the uprising of geogenic gases that could be in overpressure due to a permafrost cap (Cartwright & Harris, 1981). Soil gas composition in the MDV has been poorly investigated and essentially aimed to study biological process and temporal variability, respectively (Gregorich et al., 2006 and MacIntyre et al., 2019). To better understand the different production and migration mechanisms of gaseous species in this environment, systematic investigations are required. To date,

104 no studies have been completed to investigate the spatial distribution of soil gas linked to possible
105 fault/fracture systems, or permafrost degradation, and characterize seepage for both CO_2 and CH_4 in
106 Antarctica. Soil gas geochemistry is a useful approach that is widely used to detect diffusive/advective
107 gas emissions and identify preferential migration pathways such as buried faults and fracture systems
108 (Baubron et al., 2002; Bigi et al., 2014; Ciotoli et al., 2016; Ascione et al., 2018; Sciarra et al, 2018,
109 2019, 2021). Permafrost is generally a barrier to the migration and leakage of endogenous gaseous
110 species. However, the presence of faults and/or fractures, the thawing of the active layer and
111 permafrost degradation could allow the surface migration of anomalous concentrations of
112 endogenous gaseous species.

113 In order to investigate the possible presence of soil gas anomalies and fill the knowledge gaps
114 described above, a large-scale geochemical campaign was carried out in the MDV (i.e., in Taylor
115 Valley) during the 2019/2020 austral summer. The goal of this research is to investigate (a) the
116 composition (through soil gas survey) and (b) the potential volumes of greenhouse gasses (e.g., CO_2)
117 released atthe interface between the permafrost and active layer over a large area of Taylor Valley
118 (Fig.1). The emission rate obtained for the Lower Taylor Valley can be used for future monitoring
119 surveys and for broad extrapolations across the continent's peri-coastal zone.

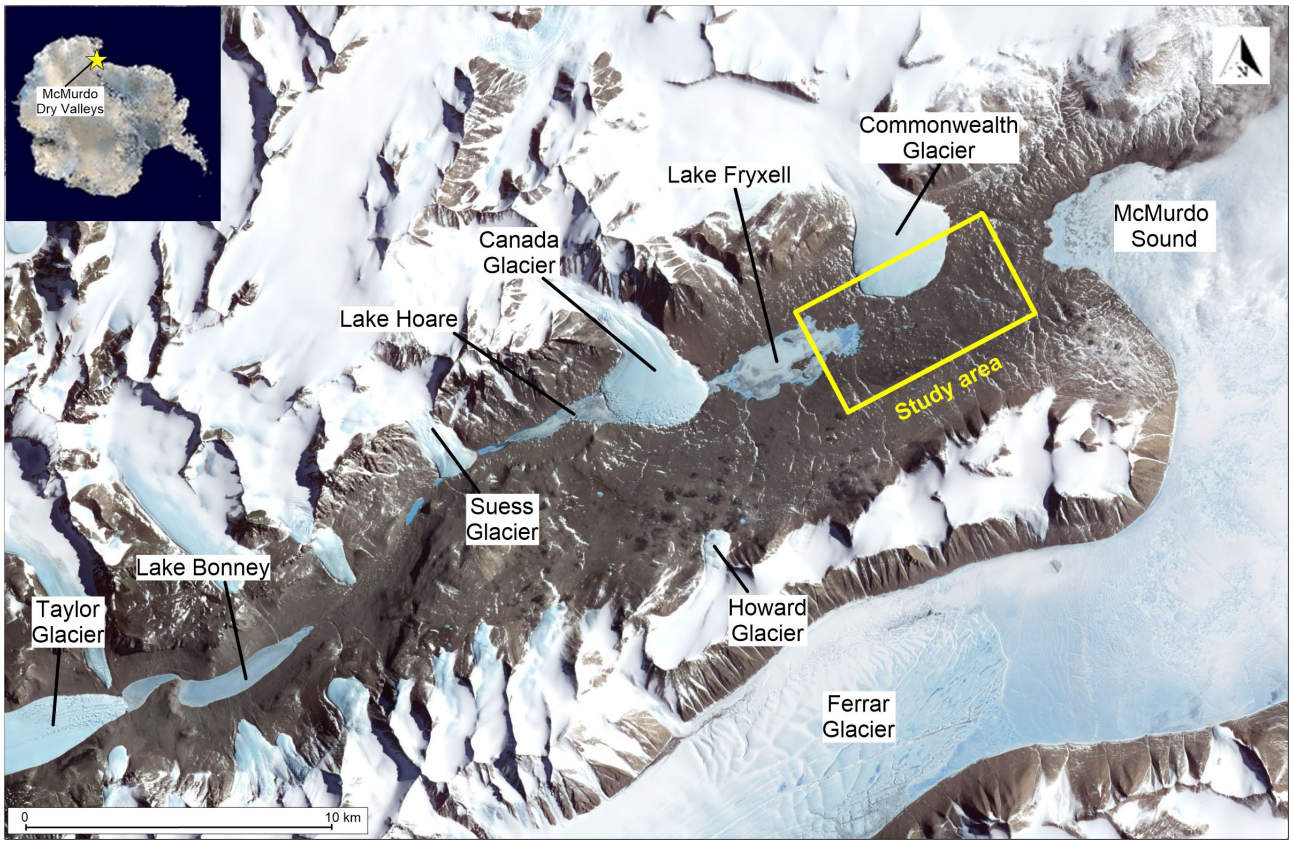

Figure 1. Location of the study area (yellow square) in Taylor Valley, McMurdo Dry Valleys, Southern Victoria Land, Antarctica. The inferred area is located among the Lake Fryxell, the Commonwealth Glacier and the McMurdo Sound. The inset indicates the location of the McMurdo Dry Valleys. (credit: NASA).

2 Methods

2.1. Site description and sampling strategy

The MDV feature a mosaic of ice-covered lakes, ponds, ephemeral streams, valley glaciers and glacial, fluvial, lacustrine and aeolian sediments (Fig. 2A). Mean annual air temperature in the MDV is −17 °C (Doran, et al 2002; Obryk et al. 2020), in particular at Lake Fryxell station over the two-year period between 2019-2020 the mean annual air temperature was - 16 ° C (Doran and Fountain, 2022), and annual precipitation (snow water equivalent) spans 3–50 mm (Fountain et al., 2010), making the MDV a cold, polar desert (Monaghen et al., 2005). Continuous permafrost, by definition, is a regional land surface with temperatures below 0°C on interannual timescales and underlies 90–

100% of the MDV. This permafrost is predominantly ice-cemented (ranging from ice-saturated to weakly cemented), although overlying "dry-frozen" (ice-free) permafrost is common in the upper ~1 m along valley walls (Bockheim et al., 2007). Massive buried ice (ground ice) is common in the MDV and has been mapped in the Quartermain Range, in Victoria Valley, and in extensive ice-cored Ross Sea drift deposits emplaced during the last glacial maximum (Hall & Denton, 2000; Bockheim et al., 2007; Swanger et al., 2010). Taylor Valley (77°37′ S, 163°15′ E) is the southernmost of the three large Dry Valleys in the Transantarctic Mountains and extends WSW-ENE for ~29 km from Taylor Glacier to McMurdo Sound (Fig. 1). Our study area is located in the eastern sector of the valley and extends for 6 km to the east of Lake Fryxell bordering the southern part of the Commonwealth Glacier (Fig. 3). The area is characterized by hummocky moraines, lacustrine deposits, and outwash fans where ephemeral streams and water tracks are active during summer. Recent studies also documented the presence of shallow underground brine systems (Mikucki et al., 2015; Foley et al., 2019). Sampling for this study was conducted according to a 250m x 250m regular grid. In the farthest areas from the expedition base camp (Fig. 2C), mainly eastern and southern sectors of the study area, the inter-distance of the samples was about 500m (Fig. 3). The sampling strategy was developed considering the logistical constraints and finalized to obtain the most representative results of the study area. Sampling was conducted as far as possible in flat/low gradient slope areas to have the same sampling conditions and to avoid gas concentrations being affected by the slope effect.

2.2 Soil gas and φCO_2 measurements

He, Ne, H_2, CH_4, CO_2 content and φCO_2 distributions were investigated to detect potential leakages from permafrost, and/or to identify the possible presence of faults and fractures, which may provide gas migration pathways.

158 Soil gas and flux surveys were carried out between December 20, 2019, and January 25, 2020. A total
159 of 157 soil gas samples (Fig. 2B) and 159 φCO_2 measurements (Fig. 2D, E) were collected in an area
160 of 21.6 km^2 with an average density of 7.3 samples/km^2.

161 Typically, soil gas samples are collected from the soil pore air by pounding a steel probe in the soil
162 at a depth of about 0.6-0.8 m (Hinkle, 1994; Beaubien et al., 2015). However, in the presence of a
163 shallow permafrost cap, our soil gas samples were collected at the bottom of the active layer that was
164 present to depths ranging between 0.15 to 0.5 m, with average depth of about 0.3 m. Elemental gas
165 composition was then analysed at Scott Base (at Pram Point on Ross Island) two weeks after
166 collection to determine the concentrations of He, Ne, H_2, O_2, N_2, CH_4, CO_2 analyses were made using
167 a MicroGC Varian 4900 CP, equipped with two Thermal Conductivity Detectors (TCD), responding
168 to the difference in thermal conductivity between the carrier gas (Ar) and the sample components.
169 The analytical error was < 3%.

170 φCO_2 amounts were measured directly in the field by using a West System™ portable fluxmeter (Fig.
171 2d, e) equipped with an IR Spectrometry detector (LICOR–LI820), with high accuracy in the range
172 from 0 up to 600 mol m^{-2} d^{-1} (0 - 26400 g m^{-2} d^{-1}). The accuracy of the measured concentration is
173 2% and the repeatability is ± 5ppm.

174 The concentration change over time is converted into CO_2 flux in g m^{-2} d^{-1} (φCO_2) considering the
175 pressure and temperature variations measured during the day, together with volume (0.0028 m^3) and
176 surface (0.0306 m^2) of the accumulation chamber, using the formula:

177 $$\varphi CO_2 = (\phi CO_2 * (86400 * P * (V/A)) / (1000000 * R * T)) * M \quad (1)$$

178 where ϕCO_2 is the soil flux expressed in ppm/sec; P is the pressure in mbar; V is volume (m^3) and A
179 is surface area (m^2) of the accumulation chamber; T is the temperature in K; M is molecular weight;
180 R = 0.08314472 in bar L $(K\ mol)^{-1}$ that is used to calculate the volume in L of an ideal gas from its
181 temperature in K, pressure in bar and mole number.

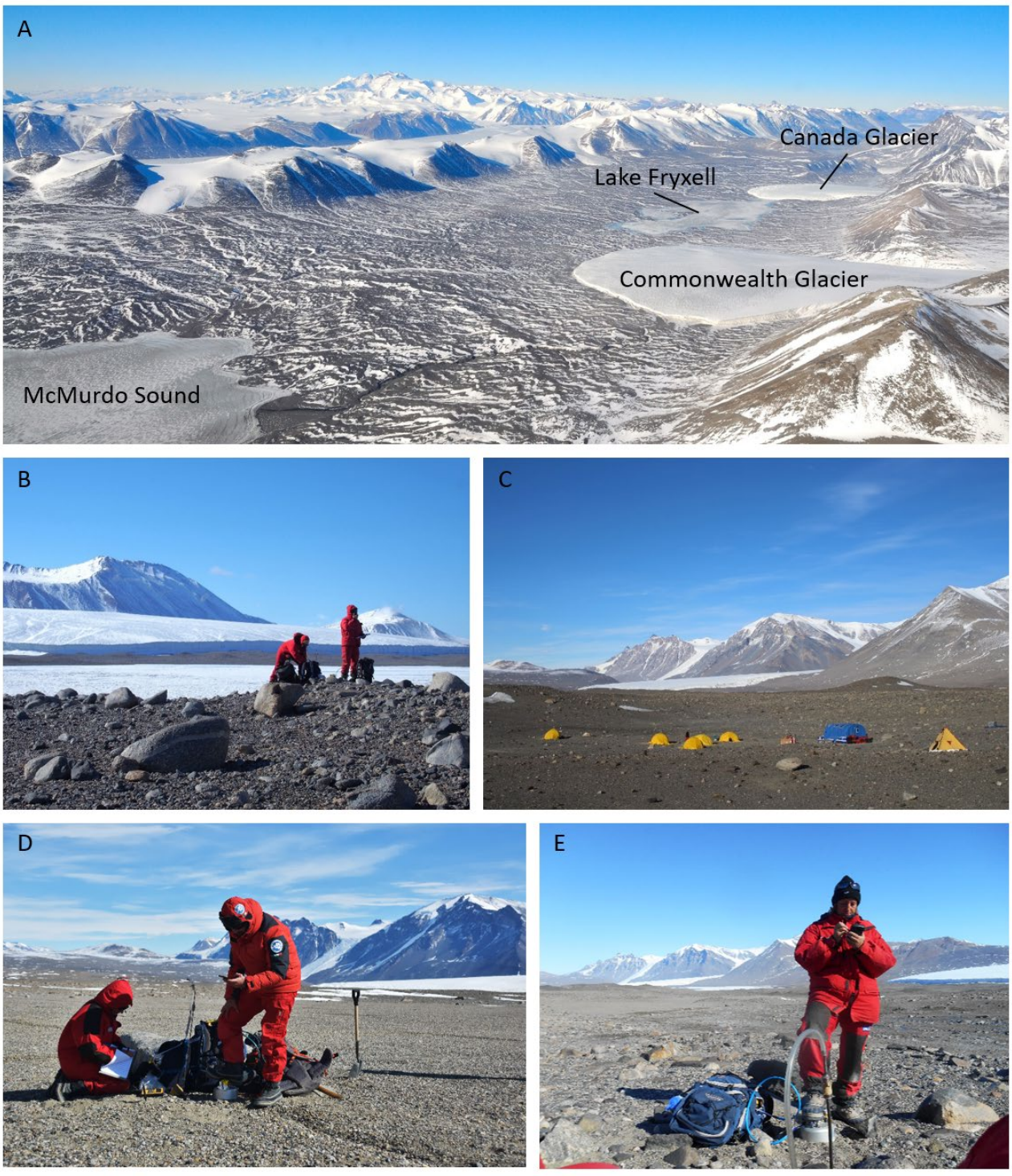

Figure 2 – View of Taylor valley from the E to W (A), soil gas sampling (B), view of the base camp (C) and detail of φCO_2 measurements (D, E).

2.3 Statistical and geostatistical analysis

187 Exploratory Data Analysis (EDA) (numerical and graphical techniques) was applied to elaborate soil
188 gas data in terms of main statistical parameters, distribution type, background, and anomalous values.
189 Normal probability plots (NPP) were interpreted according to the Sinclair method (Sinclair, 1991) in
190 order to distinguish different populations and statistical anomaly threshold values for each gas species
191 (see Fig. S1). Subsequently, geostatistical analysis (e.g., variogram analysis and kriging; Ciotoli et
192 al., 2014) was applied to construct contour maps to represent the spatial distribution of gas
193 concentrations in the surveyed area. Topographic Position Index (TPI; Jenness, 2006) has been
194 calculated to define the slope gradient of the samples by using a high-resolution Digital Elevation
195 Model (DEM; Fountain et al., 2017). Furthermore, φCO_2 measurements were used to estimate the
196 total output of CO_2 emissions from the soil to the atmosphere in the investigated area (Chiodini &
197 Frondini, 2001). This emission rate (expressed in tons day^{-1}) was calculated by multiplying the
198 average flux value of each population recognized in the NPP by the respective area estimated in the
199 contour map. The contributions of the different populations (excluding background values) where
200 then summed to obtain the total φCO_2 (see Table S1).

201

202 # 3 Results

203 ## 3.1 Soil gas composition and flux magnitude of the lower Taylor valley

204 Spatial distribution of soil gas content and flux measurements are shown in Fig. 3.

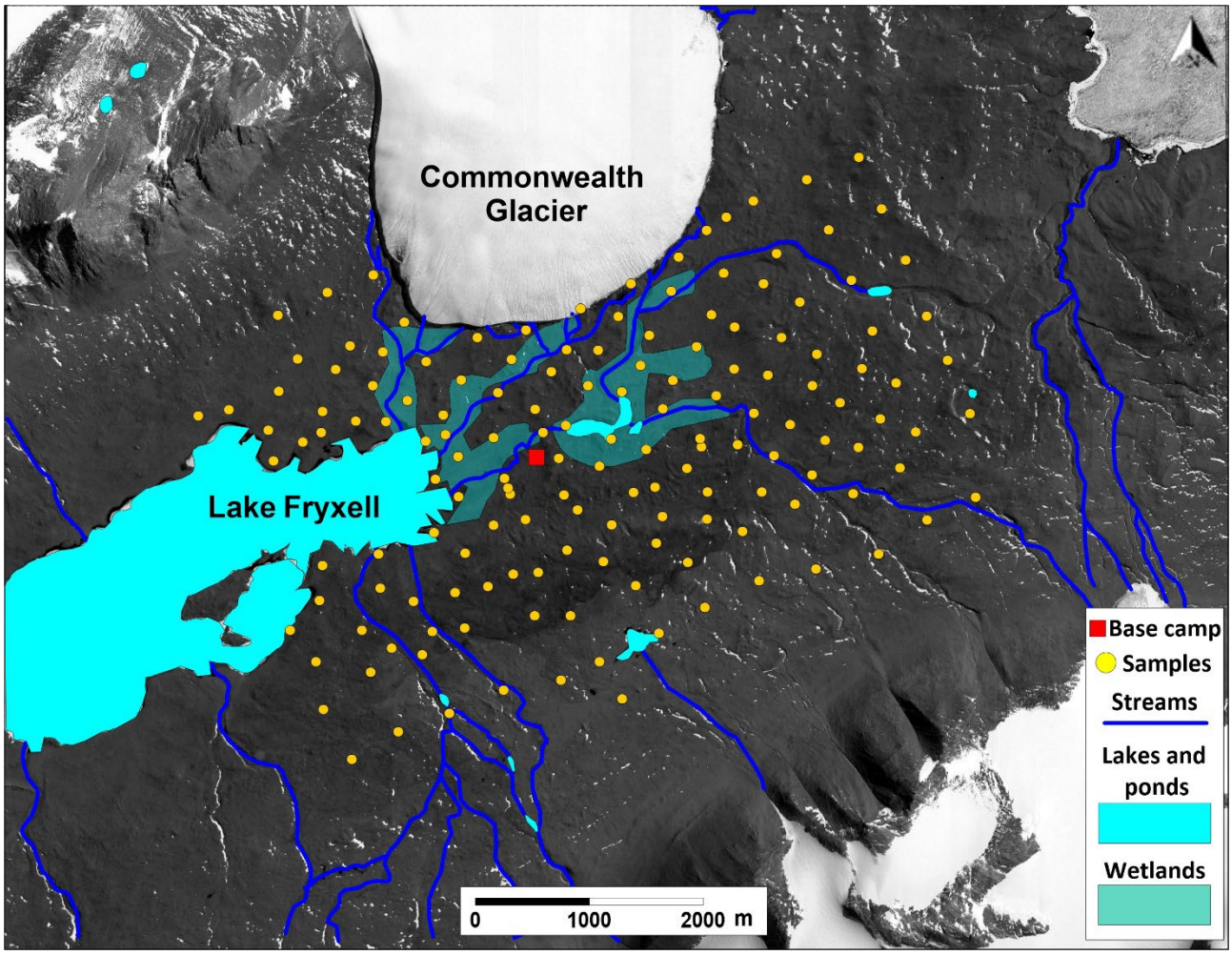

Figure 3. Location of soil gas and φCO_2 measurement points (yellow dots), of lakes and ponds (cyan areas), streams (blue lines) and wetlands (sea green areas) within Lower Taylor Valley.

The main statistics obtained for soil gas concentrations and φCO_2 are reported in Table 1. All gas species highlight broadly skewed distributions with the presence of few outliers (see SD and SK in Table 1). By comparing the mean and median values, the presence of outliers is particularly evident for H_2 and CH_4 (mean values > median values). The difference between the mean and median values also suggests a log-normal distribution for φCO_2, CO_2, CH_4 and H_2.

Table 1.
Descriptive statistics of He, Ne, H_2, O_2, N_2, CH_4, CO_2 soil gas concentration and φCO_2 measurements carried out in the Lower Taylor Valley.

	N	Mean	Median	Min	Max	LQ	UQ	P10%	P90%	SD	SK
He (ppmv)	157	5.08	5.06	4.20	6.49	5.0	5.13	4.74	5.24	0.30	1.77
Ne (ppmv)	157	17.61	17.48	15.23	22.12	17.15	17.84	16.98	18.39	0.83	2.15

H_2 (ppmv)	157	3.57	1.79	0.15	36.95	1.02	2.73	0.65	9.51	5.60	3.59
O_2 (vol%)	157	20.82	20.88	19.52	21.09	20.75	20.94	20.59	20.99	0.20	-3.07
N_2 (vol%)	157	76.18	76.25	74.23	77.19	75.95	76.54	75.50	76.77	0.53	-1.03
CH_4 (ppmv)	157	220.3	3.7	1.8	18447	3.2	4.4	2.9	25.3	1553	10.7
CO_2 (vol%)	157	0.53	0.20	0.04	3.44	0.06	0.78	0.05	1.52	0.69	2.01
φCO_2 (g $m^{-2}d^{-1}$)	159	1.73	1.20	-0.74	11.36	0.74	2.08	0.42	4.11	1.63	2.22

N: number of observations; LQ: lower quartile; UQ: upper quartile; P10%: percentile 10%; P90%: percentile 90%; SD: standard deviation; SK: skewness.

Calculated mean values are compared with the average concentrations of the same gaseous species present in the atmosphere, in the soil-atmosphere interface, and in soil gases from the available literature (Table S2) to understand the magnitude and the significance of the soil gas concentrations measured in Antarctica. In Taylor Valley, O_2, N_2 and Ne concentrations are broadly equal to their atmospheric concentration in contrast to H_2, CO_2 and CH_4 that are higher. He concentrations highlight a mean value lower than the atmospheric concentration (5.22 ppmv), and as evidenced by the 90% percentile, as only less than 10% of the total samples shows higher concentrations than the atmosphere.

N_2, O_2 and Ne concentrations (76.2 vol%, 20.8 vol% and 17.6 ppmv, respectively; Table 1) highlight atmospheric origin as confirmed by the N_2/O_2 ratio (~ 3.8). This value is different from those detected in ice bubbles (up to 6; Ikeda-Fukazawa et al., 2001) or dissolved gas from groundwater, together with the lack of O_2 depletion, highlights that N_2, O_2 and Ne are linked to the overlying air diffusing downward into the soil column. Otherwise, the linear trend of the samples in the scatterplot of Fig. 4 shows the existence of a dilution process of atmospheric gases (N_2 and O_2) by CO_2 (dashed line). This effect leads to exclude a biological or atmospheric contribution to the soil system but may be linked to a different intake of CO_2, for example, a deep geological CO_2 contribution (Romanak et al., 2012). An in-situ consumption of O_2 (e.g., biological/chemical reactions) shown by the stoichiometric 1:1 (black solid line) decrease in oxygen is not obviously present.

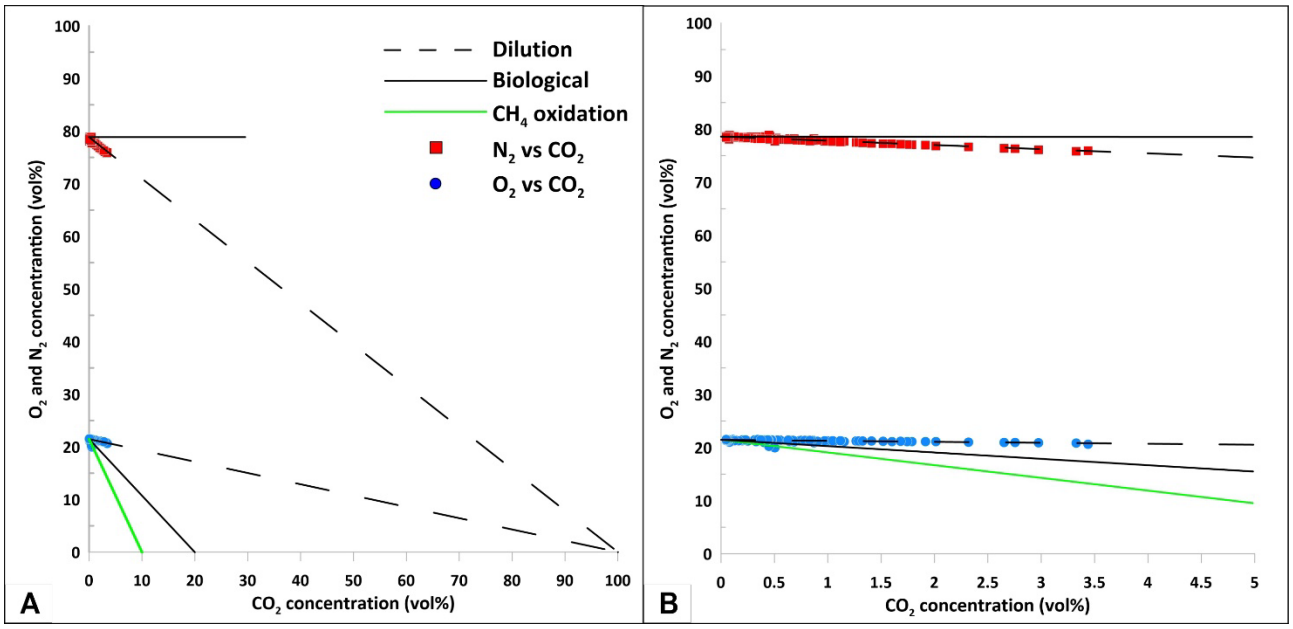

Figure 4. (A) Scatter plot of O_2 and N_2 vs CO_2 (concentrations, vol%). The correlations between nitrogen and carbon dioxide, as well as oxygen and carbon dioxide, provide information about the trend of data. Black solid lines highlight a biological source for the CO_2. Green lines show CO_2 derived by CH_4 oxidation, while dashed lines indicate a dilution, an external contribution of CO_2 into the soil closed system. (B) The same plot showing CO_2 concentrations up to 5%.

3.2 Spatial distribution of soil gas concentrations and φCO_2 values

The analysis of samples' position versus slope (TPI slope position, Fig. S2) reveals that more than 60% of the data fall within the middle slope class (Table S3), in this way we limited slope influence on the measured gas concentration. NPPs highlighted the following anomaly threshold values: 5.4 ppmv for He, 18.8 ppmv for Ne, 4 ppmv for H_2, 9 ppmv for CH_4, 0.5 vol% for CO_2 and 3 $gm^{-2}d^{-1}$ for φCO_2. In Fig. 5A, CH_4 spatial distribution shows higher values (up to 18,447 ppmv) in the NE and E sectors, and weak anomalies (between background and anomaly) in the other sectors except for the central part of the study area where only background values occur. The contour map of CO_2 (Fig. 5B) shows diffuse anomalous values (up to 3.44 vol%) to the S, SW and central sectors of the study area, while in the E sector background values dominate. Some weak CO_2 anomalies are consistent with CH_4 anomalies, suggesting a common source for these gases and the same migration mechanisms towards the surface. The spatial distribution of φCO_2 is shown in Fig. 5C. The main anomalies are observed in the NE and SE sectors, in the central south part, and weak ones are also present in the

SW sector. H_2 distribution (Fig. 5D) shows small anomalous values scattered throughout the study area. However, some of the H_2 anomalies correspond with those observed for CH_4 and CO_2. Regions with high He concentrations (Fig. 5E) are distributed along N and S borders of the study area. Ne concentrations (Fig. 5F) largely increase together with He and are mostly located along the N edge of the study area.

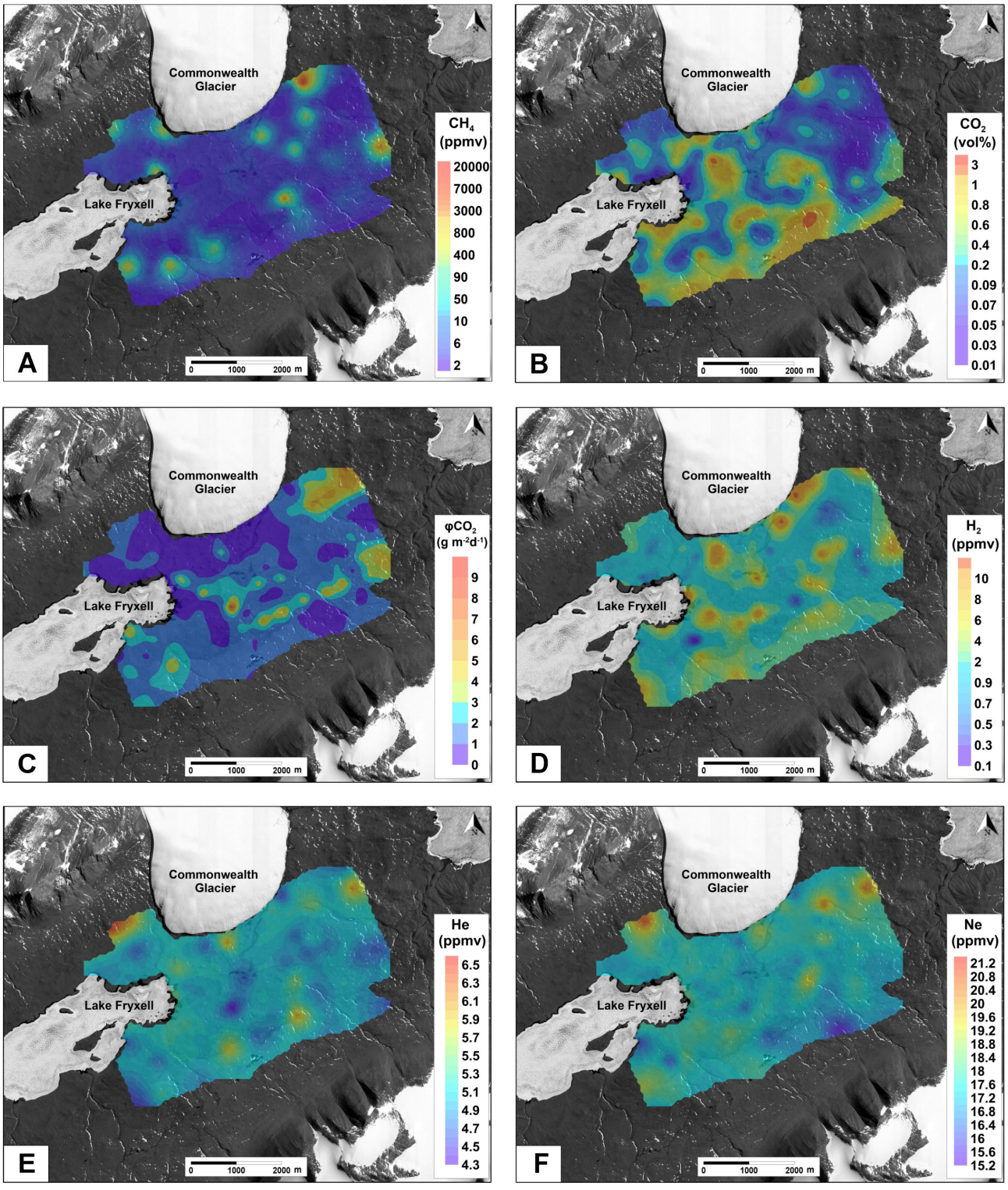

Figure 5. Contour maps of the analysed gas species and the φCO_2. The figure shows the spatial distribution of CH_4 concentrations (A), CO_2 concentrations (B), φCO_2 (C), H_2 concentrations (D), He concentrations (E) and Ne concentrations (F).

The distribution of the positive anomalies for CH_4, CO_2, H_2 and φCO_2 are consistent in the NE, NW and S sectors, while He shows a good correlation with CO_2 and CH_4 anomalies in the S and N sectors, respectively (Fig. 5). The detection of helium in shallow soil is generally indicative of deep sources (Baubron et al., 2002; Sciarra et al., 2021), and is typically associated with high concentrations of CO_2 and CH_4 that act as carrier gas for trace gases (e.g., He, ^{222}Rn; Ciotoli et al., 2007; Ascione et al., 2018). Indeed, these trace gases (like radon, hydrogen and helium, often together with other gas like CO_2 and CH_4) are successfully used as pathfinder component to discover buried fault and fracture fields, mostly when other conventional structural-geology methods are lacking or unreliable (e.g., Sciarra et al., 2021 and references therein). Indeed, the spatial distribution of soil gasses in faulted/fractured areas appears to be a suitable tool for identifying active structures that act as preferential leakage pathways. The migration of these gases by diffusion and/or advection along buried active faults/fractures can generate shallow anomalies with concentrations significantly higher than background levels; these anomalies can provide reliable information about the location and the geometry of the shallow fracturing zone, as well as about the permeability within the fractured zone.

The source of these gas anomalies could be linked with the over pressurized (Cartwright & Harris, 1981) brine system flowing under Taylor Valley (Mikucki et al., 2015; Foley et al., 2019) that during summer periods can release dissolved gases after active layer thawing/permafrost degradation. These gases can then easily migrate toward the surface through permeable layers, as well as local fractures and/or buried faults or permafrost lateral discontinuities (e.g., permafrost/bedrock contact at the edges of the valley). These may act as preferential migration pathways (Ciotoli et al., 2007; Ascione et al., 2018; Sciarra et al., 2019) thus resulting in the linear multigas anomalous zones observed in the study area (pink zones in Fig. 6). These gas anomalies are aligned in ENE-WSW direction in the S and N sectors of the study area, respectively. In the northernmost sector of the studied area, the anomalous zone does not appear as continuous as that occurring in the southern sector, due to the presence of the Commonwealth Glacier and related wetlands and streams (Fig. 3). These systems, being richer in water content, probably prevent gas upwelling, creating a sealing effect.

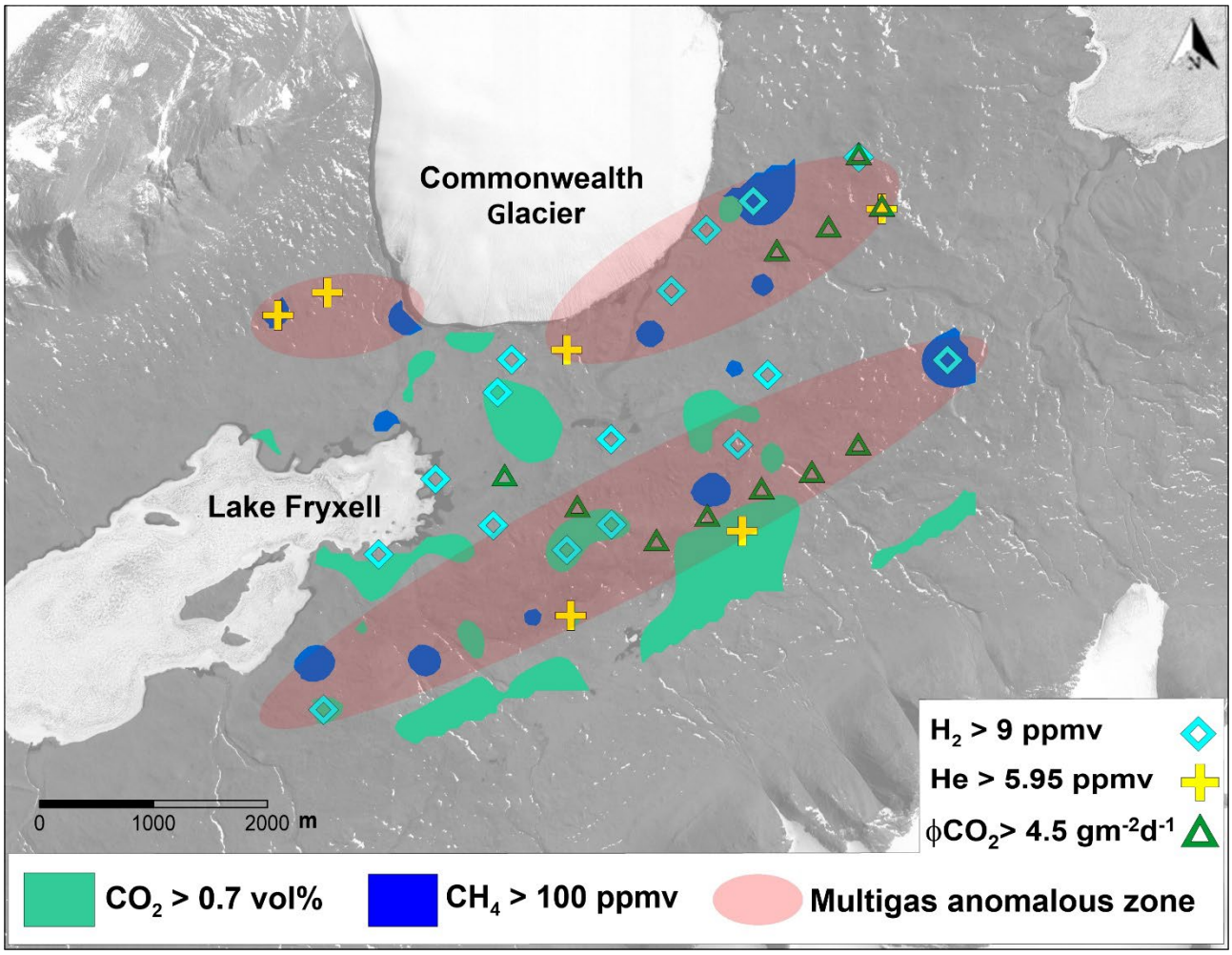

Figure 6. The map shows contour areas of CO_2 (green) and CH_4 (blue) concentrations higher than 0.7 vol% and 100 ppmv, respectively, samples with H_2 higher than 9 ppmv (light blue rhombuses), He higher than 5.95 ppmv (yellow crosses), φCO_2 higher than 4.5 g $m^{-2}d^{-1}$ (green triangles). The multigas anomalous zones are shown by the pink ellipsoids.

As for the southern sector, there are also two physical factors that may increase permafrost degradation: solar radiation and soil albedo. Solar radiation is more intense on the North facing slopes than on the South facing ones and, in summertime the soil temperatures increase in the former (Fountain et al., 2014; Lacelle et al., 2016). On the southern slope, south of Commonwealth Glacier is an area rich in dark basalt and anorthoclase phonolite (Murrell, 1973). Campbell et al. (1998) found the greatest heating on dark coloured basalt soils. The combination of these phenomena may enhance the superficial degradation of the permafrost in the southern sector (i.e., where the major gaseous anomalies have been identified).

4 Discussion

In the MDV, very limited prior datasets are available for soil gas concentrations of CO_2, CH_4 and N_2. In the 2003-2005 austral summers, Gregorich et al. (2006) measured up to 0.55 vol% of CO_2 and up to 5780 ppmv of CH_4 in Garwood Valley. In January 2014, MacIntyre et al. (2019) measured a maximum value of 0.044 vol% of CO_2 in the Lower Taylor Valley, near Howard Glacier (Fig.1). Both studies found CO_2 concentrations 1-2 orders of magnitude lower than the maximum value measured in this study (3.44 vol%, Table 1). The highest CH_4 value reported in Gregorich et al. (2006) is in the same order of magnitude as found in this study, although more than three times lower than our maximum value (18,447 ppmv, Table 1). Both previous studies, collected a limited number of measurements and focused on temporal variability rather than spatial variability. Worldwide, CO_2 and CH_4 soil gas data are numerous, and measured in different environments: in the Arctic Finnish Lapland, Voigt et al. (2019), measured CO_2 max value of about 6 vol% and CH_4 max value of about 300 ppmv. In Italy, for example, where a database with over 10,000 soil gas measurements is available, Ciotoli et al. (2014) reported CO_2 mean values for 3 different geological scenarios: about 3 vol% for Tyrrhenian basins, 1.57 vol% for Apennine Intermontane plains and 1.09 vol% for foredeep basins.

In contrast, φCO_2 measurements have been conducted in Antarctica since 1994 (see Table 2). The φCO_2 measurements in the study presented herein are up to three orders of magnitude higher than previous studies, therefore, the highest measured in the MDV. φCO_2 measurements in this work in Taylor Valley are on average comparable with the values measured in the Arctic (Burkins et al, 2001), sub-Arctic (Turetsky et al., 2002), desert (Burkins et al., 2001; Mazzini et al., 2019) and alpine (Sommerfeld et al., 1993) areas and lower than other areas of the globe (Oechel et al, 1993; Burkins et al., 2001).

Table 2.

Summary table of φCO_2 measured in different terrestrial environments. Soil emission rates in g m^{-2} d^{-1} from Antarctic, Arctic, and other ecosystems (e.g., Alpine and sub-alpine, Mediterranean, desert and tropical climates).

Study site	Date	CO_2 rate (g $m^{-2}d^{-1}$)	Reference
Antarctic			
Taylor Valley	1994-1997	0.1	Burkins et al., 2001
Ross Sea	1997-2003	-0.35 — -0.02	Arrigo and Van Dijken, 2007
Lake Fryxell, Taylor Valley	2001-2002	-0.3 — 0.57	Parsons et al., 2004
Lake Hoare, Taylor Valley	2001-2002	-0.38 — 0.42	Parsons et al., 2004
Lake Bonney, Taylor Valley	2001-2002	0.004 — 0.08	Parsons et al., 2004
Upper moraine; Garwood Valley	2003	0.0005	Elberling et al., 2006
Delta; Garwood Valley	2003	0.0006	Elberling et al., 2006
Sand dune; Garwood Valley	2003	0.00045	Elberling et al., 2006
Lower moraine; Garwood Valley	2003	0.0009	Elberling et al., 2006
Polygons; Garwood Valley	2003	0.0007	Elberling et al., 2006
Hill slope; Garwood Valley	2003	0.0008	Elberling et al., 2006
Stream edge; Garwood Valley	2003	0.0024	Elberling et al., 2006
Lake edge; Garwood Valley	2003	0.0137	Elberling et al., 2006
Garwood Valley	2003	0.9504	Gregorich et al., 2006
Garwood Valley	2005	1.59	Gregorich et al., 2006
Lake Mochou	2007-2008	-1.70	Zhu et al., 2010
Lake Tuanjie	2007-2008	-0.89	Zhu et al., 2010
Taylor Valley	2008-2009 h13:00-15:00	0.097	Shanhun et al., 2012
Taylor Valley	2008-2009 h06:00-08:00	-0.09	Shanhun et al., 2012
Hidden Valley	2011	0.02 – 1.56	Risk et al., 2013
Taylor Valley	*2019-2020*	*1.73*	*This work*
Arctic			
Subarctic fens, Canada	-	0.09 — 1.28	Moore and Knowles, 1987
Bog, Canada	-	0.05	Vitt and Chee, 1990
Poor fen, Canada	-	0.17	Vitt and Chee, 1990
Drained swamp peatlands, Canada	-	0 — 0.016	Shannon et al., 1993
Toolik Lake, Alaska	-	0.15 — 0.78	Oechel et al., 1993
Arctic tundra	-	1.59	Burkins et al., 2001
Boreal peatland, Canada	-	0.08	Turetsky et al. 2002
Other ecosystems			
Sub-alpine snowpack	-	2.046	Sommerfeld et al., 1993
Alpine snowpack	-	0.693	Sommerfeld et al., 1993
Desert scrub soil	-	0.59	Burkins et al., 2001
Deciduous forest soil	-	2.5	Burkins et al., 2001
Tropical soil	-	3.34	Burkins et al., 2001
Temperate	-	1.9 - 30.41	Oertel et al., 2016
Mediterranean	-	1.9 - 10.26	Oertel et al., 2016
Subtropical	-	2.66 - 4.94	Oertel et al., 2016
Rocky Desert	-	6.17	Mazzini et al., 2019

Although carbon isotope and radiocarbon analyses would strengthen the hypothesis on the origin and age of carbon, from a geological point of view, various authors have identified in the soil, in correspondence with faults and particularly fractured areas, concentrations of different gases and CO_2 fluxes higher than those given by simple soil respiration. From these studies it appears that the presence in anomalous concentrations of CO_2 (but also CH_4, ^{222}Rn and He) derives from a combination of the biological component and endogenous contributions. Our study is exclusively focused on the endogenous contribution linked to geogenic processes.

Previous studies, linked the origin of CO_2 in Antarctic soils to biological activity, favoured by soil alkalinity and by shallow abiotic processes (CO_2 solubility), soil moisture content and soil temperature variations (Parsons et al., 2004; Elberling et al., 2006; Gregorich et al., 2006; Ball et al., 2009; MacIntyre et al., 2019). Shanhun et al. (2012) and Risk et al. (2013), however, suggested an abiotic origin of CO_2 based on the isotopic analyses, reporting very high positive φCO_2 values that cannot be explained by normal microbial activity, also considering the typical dry valley soils characterized by low organic C contents (<1 mg g^{-1}). We suggest that the measured high anomaly values, originate from the subsurface brine system (Mikucki et al., 2015; Foley et al., 2019), and are linked to permafrost cap discontinuities at the edges of the valley (fractures, buried local faults or bedrock contact). The spatial distribution of these anomalous zones could also be locally influenced by shallow active layer thawing and/or permafrost degradation.

While the samples were collected at shallow depths (i.e., the top layer of the permafrost is often present at 30 cm depth) and are potentially affected by atmospheric gas dilution (Hinkle, 1994; Beaubien et al., 2015), the anomalous values of He, CH_4, CO_2 and φCO_2 cannot completely be explained by biological activity and/or superficial physical processes. Another aspect concerns the presence of soil moisture which prevents both sampling and gas rising (Hinkle, 1994; Beaubien et al., 2015). In Taylor Valley, the wetlands represent an area where water permeates the pores of the soil but does not emerge on the surface. Within these areas (about 2.1 km^2, i.e., equal to 10% of the total study area), we managed to complete 16 soil gas samples and φCO_2 (Fig. 3). However, it should be

noted that the gas concentrations are certainly underestimated compared to those conducted in dry and ventilated soil conditions as confirmed by statistical analyses (Table S4).

Figure 7 is a compilation of the ranges and average values of φCO_2 measured over time in Antarctica. It should be noted that the reported measurements were conducted using various methods and in different environments, e.g., there are measurements on dry soil, near and far from lakes and from the Ross Sea. The average value of our data is in the same order of magnitude of those reported from the Garwood Valley (Gregorich et al., 2006). The maximum values measured in Gregorich et al. (2006) and our study, is at least one order of magnitude higher than those previously reported in Antarctica. Our measurements values are two orders of magnitude greater than those previously measured in the Taylor Valley (Burkins et al., 2001; Parsons et al., 2004; Shanhun et al., 2012).

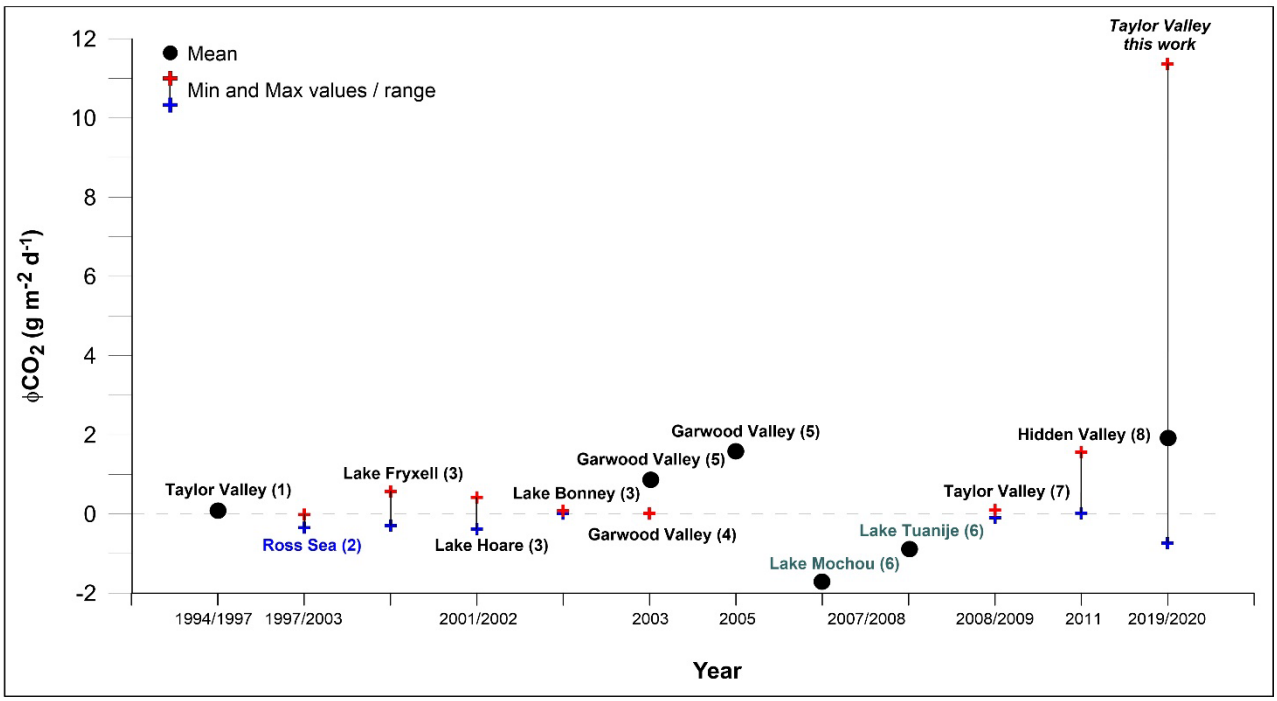

Figure 7. Summary diagram of φCO_2 measurements carried out since 1994 in Antarctica. The diagram shows CO_2 measurements performed in Antarctica by using various methods and in different environments. Measurements on dry soil (in black), lakes (in light blue) and the Ross Sea (in blue) are reported. References: 1 Burkins et al., 2001; 2 Arrigo and Van Dijken, 2007; 3 Parsons et al., 2004; 4 Elberling et al., 2006; 5 Gregorich et al., 2006; 6 Zhu et al., 2010; 7 Shanhun et al., 2012; 8 Risk et al., 2013.

382 The total CO_2 gas emission rates over the surveyed area (A = 21.6 km^2) have been computed
383 following a statistical approach (see 2.3 Statistical and geostatistical analysis) and, the calculated
384 average CO_2 output is ~15 tons day^{-1} (Table S1) which is estimated to count for a total of 1,345 tons
385 released during the three summer months. This value can be also considered as the total annual CO_2
386 emitted, providing a conservative estimate for the warmest months expecting much lower emissions
387 during the rest of the year. Therefore, the estimated emission factor in the study area is 62 tons km^{-2}
388 y^{-1}. Although our emission value is low, forecasting that ice-free regions in Antarctica are likely to
389 expand with gradual warming, this amount will tend to increase and should be counted in the global
390 CO_2 budget estimations.

391

392 # 5 Conclusions

393 The main objective of this study was to detect the presence of degassing in permafrost bearing region
394 and to evaluate the migration mechanisms along different permeability pathways.

395 We provide the first unedited spatial distribution maps of soil gas concentrations and φCO_2 over a
396 large area (> 20 km^2) of Taylor Valley, Antarctica. 157 soil gas samples were collected and analysed
397 allowing two gas categories to be identified based on their composition. We found atmospheric values
398 of O_2, N_2 and Ne, probably related to the overlying air that spreads down the column of the soil, and
399 anomalous values of CO_2 (up to 3.44 vol%) causing a dilution of atmospheric gases due to an upward
400 flux of deep carbon dioxide. We also detected high and anomalous values of CH_4 (up to 18,447
401 ppmv), He (up to 6.49 ppmv) and H_2 (up to 32.95 ppmv), supporting the presence of buried gas-
402 bearing channels where the CO_2 migration acts as carrier for trace species (e.g., He, H_2), suggesting
403 a potentially deep origin of these gases. This hypothesis is strengthened where methane and helium
404 anomalies are also measured. The calculated CO_2 emissions during the summer period is 1,345.5 tons
405 for 90 days (summertime) for the whole studied area. The collected data identified areas characterized

406 by multigas anomalies where active layer melting occurs during the summer period and where fluids
407 migrate to the surface through structures/fractures or permafrost lateral discontinuities aligned with
408 the main direction of the valley. We suggest that the gases originate from the subsurface over
409 pressurized brine system that is probably rich in dissolved gasses. The superficial melting of the active
410 layer/permafrost degradation and the presence of permeable zones inside the permafrost cap, allowed
411 these gases to migrate to the surface. Here we report the highest concentrations of GHGs measured
412 in an Antarctic region that previously considered to be a CO_2 sink. Our results show that these soils
413 have already begun to degas; this phenomenon may not be limited to Taylor Valley alone but extend
414 to all the more than 24,000 km of coastline of the Antarctic continent in the future. Our results
415 emphasize that extensive surveys are necessary to properly evaluate greenhouse gas emissions in
416 regions with permafrost. The established baseline maps produced during this expedition can be used
417 to compare future monitoring soil gas concentrations and CO_2 emissions in the region.

418

419 **References**

420 1. Adams, B.J., Bardgett, R.D., Ayres, E., Wall, D.H., Aislabie, J., Bamforth, S., Bargagli, R.,
421 Cary, C., Cavacini, P., Connell, L., Convey, P., Fell, J.W., Frati, F., Hogg, I.D., Newsham,
422 K.K., O'Donnell, A., Russell, N., Seppelt, R.D., Stevens, M.I., 2006. Diversity and
423 distribution of Victoria Land biota. Soil Biol. Biochem. 38, 3003–3018.
424 https://doi.org/10.1016/J.SOILBIO.2006.04.030
425 2. Anthony, K. M. W., Anthony, P., Grosse, G., & Chanton, J., 2012. Geologic methane seeps
426 along boundaries of Arctic permafrost thaw and melting glaciers. Nat. Geosci. 5, 419-426.
427 3. Arrigo, K.R., & Van Dijken, G.L, 2007. Interannual variation in air-sea CO_2 flux in the Ross
428 Sea, Antarctica: A model analysis. J. Geophys. Res.: Oceans, 112.
429 4. Ascione, A., Ciotoli, G., Bigi, S., Buscher, J., Mazzoli, S., Ruggiero, L., Sciarra, A.,
430 Tartarello, M.C., and Valente, E., 2018. Assessing mantle versus crustal sources for non-
431 volcanic degassing along fault zones in the actively extending southern Apennines mountain
432 belt (Italy). GSA Bullettin Data Repository item 2018150. https://doi.org/10.1130/B31869.1

5. Ball, B.A., Virginia, R.A., Barrett, J.E., Parsons, A.N., Wall, A.H., 2009. Interactions between physical and biotic factors influence CO_2 flux in Antarctic dry valley soils. Soil Biol. Biochem. 41, 1510-1517.
6. Barrett, J.E., Virginia, R.A., Wall, D.H., Cary, S.C., Adams, B.J., Hacker, A.L., Aislabie, J.M., 2006. Co-variation in soil biodiversity and biogeochemistry in northern and southern Victoria Land, Antarctica. Antarct. Sci. 18, 535.
7. Baubron, J.-C., Rigo, A., Toutain, J.-P., 2002. Soil gas profiles as a tool to characterize active tectonic areas: The Jaut Pass example (Pyrenees, France). Earth Planet. Sci. Lett. 196, 69–81.
8. Beaubien, S. E., Ruggiero, L., Annunziatellis, A., Bigi, S., Ciotoli, G., Deiana, P Graziani S., Lombardi S., Tartarello, M. C., 2015. The importance of baseline surveys of near-surface gas geochemistry for CCS monitoring, as shown from onshore case studies in northern and southern Europe. Oil Gas Sci. Technol. 70, 615-633 (2015).
9. Bigi S., Beaubien S.E., Ciotoli G., D'Ambrogi C., Doglioni C., Ferrante V., Lombardi S., Milli S., Orlando L., Ruggiero L., Tartarello M.C., Sacco P., 2014. Mantle-derived CO_2 migration along active faults within an extensional basin margin (Fiumicino, Rome, Italy). Tectonophysics 637, 137-149.
10. Bockheim, J.G., Campbell, I.B., McLeod, M., 2007. Permafrost distribution and active-layer depths in the McMurdo Dry Valleys, Antarctica. Permafr. Periglac. Process 18, 217–227.
11. Burke, E. J., Ekici, A., Huang, Y., Chadburn, S. E., Huntingford, C., Ciais, P., Friedlingstein P., Shushi Peng S., Krinner, G., 2017. Quantifying uncertainties of permafrost carbon–climate feedbacks. Biogeosciences 14, 3051-3066.
12. Burkins, M.B., Virginia, R.A., Wall, D.H., 2001. Organic carbon cycling in Taylor Valley, Antarctica: quantifying soil reservoirs and soil respiration. Glob. Chang. Biol. 7, 113–125.
13. Campbell, I.B., & Claridge, G.G., 2009. Antarctic permafrost soils. In Permafrost soils. (Springer, Berlin, Heidelberg, pp. 17-31.
14. Campbell, I.B., Claridge, G.G.C., Campbell, D.I., & Balks, M.R., 1998. Permafrost properties in the McMurdo Sound Dry Valley Region of Antarctica. Proceedings In Seventh International Conference on Permafrost, Yellowknife (Canada), Collection Nordicana 55, 121-126.
15. Cartwright, K., & Harris H.J.H., 1981. Hydrogeology of the dry valley region Antarctica Antarctic Research Series, Dry Valley Drilling Project, Vol. 33, 193-214.
16. Chapman, W.L., Walsh, J.E., 2007. A synthesis of Antarctic temperatures. J. Clim. 20, 4096–4117.

17. Chiodini, G., & Frondini, F., 2001. Carbon dioxide degassing from the Albani Hills volcanic region, Central Italy. Chem. Geol. 177, 67-83.
18. Ciais, P., Sabine C., Bala G., Bopp L., Brovkin V., Canadell J., Chhabra A., DeFries R., Galloway J., Heimann M., Jones C., Le Quéré C., Myneni R.B., Piao S., Thornton P., 2013. Carbon and Other Biogeochemical Cycles. In: Climate Change 2013: The Physical Science Basis. Contribution of Working Group I to the Fifth Assessment Report of the Intergovernmental Panel on Climate Change Editor: Stocker, T.F. et al. Cambridge University Press, Cambridge, United Kingdom and New York, NY, USA, pp. 465–570, doi:10.1017/CBO9781107415324.015
19. Ciotoli, G., Lombardi, S., & Annunziatellis, A., 2007. Geostatistical analysis of soil gas data in a high seismic intermontane basin: Fucino Plain, central Italy. J. Geophys. Res. Solid Earth 112(B5).
20. Ciotoli, G., Bigi, S., Tartarello, C., Sacco, P., Lombardi, S., Ascione, A., & Mazzoli, S., 2014. Soil gas distribution in the main coseismic surface rupture zone of the 1980, Ms= 6.9, Irpinia earthquake (southern Italy). J. Geophys. Res. Solid Earth 119, 2440-2461.
21. Ciotoli, G., Etiope, G., Marra, F., Florindo, F., Giraudi, C., & Ruggiero, L., 2016. Tiber delta CO_2-CH_4 degassing: a possible hybrid, tectonically active sediment-hosted geothermal system near Rome. J. Geophys. Res. Solid Earth 121, 48-69.
22. Cory, R.M., Ward, C.P., Crump, B.C., & Kling, G.W., 2014. Sunlight controls water column processing of carbon in arctic fresh waters. Science 345, 925–928.
23. Doran, P.T., McKay, C.P., Clow, G.D., Dana, G.L., Fountain, A.G., Nylen, T. and Lyons, W.B., 2002. Valley floor climate observations from the McMurdo Dry Valleys, Antarctica, 1986 - 2000. Journal of Geophysical Research, 107, 4772-4784
24. Doran, P.T. and Fountain, A.G., 2022. High frequency measurements from Lake Fryxell Meteorological Station (FRLM), McMurdo Dry Valleys, Antarctica (1993-2021, ongoing). Environmental Data Initiative. DOI: 10.6073/pasta/0f81d6d9c2b0f6ee9e7151db57733aec
25. Elberling, B., Gregorich, E.G., Hopkins, D.W., Sparrow, A.D., Novis, P., Greenfield, L.G., 2006. Distribution and dynamics of soil organic matter in an Antarctic dry valley. Soil Biol. Biochem. 38, 3095-3106.
26. Faucher, B., Lacelle, D., Davila, A., Pollard, W., Fisher, D., and McKay, C.P., 2017. Physicochemical and Biological Controls on Carbon and Nitrogen in Permafrost from an Ultraxerous Environment, McMurdo Dry Valleys of Antarctica. J. Geophys. Res. Biogeosci. 122, 2593–2604.

27. Foley, N., Tulaczyk, S. M., Grombacher, D., Doran, P. T., Mikucki, J., Myers, K. F., Foged N., Dugan H., Auken E. & Virginia, R., 2019. Evidence for pathways of concentrated submarine groundwater discharge in east Antarctica from helicopter-borne electrical resistivity measurements. Hydrology 6, 54. https://doi.org/10.3390/hydrology6020054
28. Fountain, A.G., Fernandez-Diaz, J.C., Obryk, M., Levy, J., Gooseff, M., Van Horn, D.J., Morin, P., & Shrestha, R., (2017), High resolution elevation mapping of the McMurdo Dry Valleys, Antarctica, and surrounding regions, Earth Syst. Sci. Data, 9, 435-443.
29. Fountain, A.G., Levy, J.S., Gooseff, M.N., & Van Horn, D., 2014. The McMurdo Dry Valleys: a landscape on the threshold of change. Geomorphology 225, 25-35.
30. Fountain, A.G., Nylen, T.H., Monaghan, A., Basagic, H.J., Bromwich, D., 2010. Snow in the McMurdo Dry Valleys, Antarctica. Int. J. Climatol. 30, 633–642.
31. Gilichinsky, D.A., Wilson, G.S., Friedmann, E.I., McKay, C.P., Sletten, R.S:, Rivkina. E.M., Vishnivetskaya, T.A., Erokhina, L.G., Ivanushkina, N.E., Kochkina, G.A., Shcherbakova, V.A., Soina, V.S., Spirina, E.V., Vorobyova, V.A., Fyodorov-Davydov, D.G., Hallet, B., Ozerskaya, S.M., Sorokovikov, V.A., Laurinavichyus, K.S., Shatilovich, A.V., Chanton, J.P., Ostrounov, V.E., and Tiedje, J.M., 2007. Microbial Populations in Antarctic Permafrost: Biodiversity, State, Age, and Implication for Astrobiology. Astrobiology, 7 (2), 275-311. doi: 10.1089/ast.2006.0012
32. Gregorich, E.G., Hopkins, D.W., Elberling, B., Sparrow, A.D., Novis, P., Greenfield, L.G., Rochette, P., 2006. Emission of CO_2, CH_4 and N_2O from lakeshore soils in an Antarctic dry valley. Soil Biol. Biochem. 38, 3120–3129. https://doi.org/10.1016/J.SOILBIO.2006.01.015
33. Gruber, S., 2012. Derivation and analysis of a high-resolution estimate of global permafrost zonation, The Cryosphere, 6, 221–233. https://doi.org/10.5194/tc-6-221-2012
34. Hagedorn, B., Sletten, R.S., Hallet, B., 2007. Sublimation and ice condensation in hyperarid soils: modeling results using field data from Victoria Valley, Antarctica. J. Geophys. Res. 112, F03017.
35. Hall, B.L., Denton, G.H., 2000. Radiocarbon chronology of Ross Sea drift, eastern Taylor Valley, Antarctica: evidence for a grounded ice sheet in the Ross Sea at the last glacial maximum. Geogr. Ann. 82A, 305–336.
36. Hinkle, M. E., 1994. Environmental conditions affecting concentrations of He, CO_2, O_2 and N_2 in soil gases. Appl. Geochem. 9, 53-63.
37. Hopkins, D.W., Sparrow, A.D., Elberling, B., Gregorich, E.G., Novis, P.M., Greenfield, L.G., Tilston, E.L., 2006. Carbon, nitrogen and temperature controls on microbial activity in soils

from an Antarctic dry valley. Soil Biol. Biochem. 38, 3130–3140. https://doi.org/10.1016/J.SOILBIO.2006.01.012

38. Ikeda-Fukazawa, T., Hondoh, T., Fukumura, T., Fukazawa, H., & Mae, S., 2001. Variation in N_2/O_2 ratio of occluded air in Dome Fuji Antarctic ice. Journal of Geophysical Research: Atmospheres, 106(D16), 17799-17810.
39. Jenness, J. 2006. Topographic Position Index (tpi_jen.avx) extension for ArcView 3.x, v. 1.2. Jenness Enterprises. Available at: http://www.jennessent.com/arcview/tpi.htm.
40. Lacelle, D., Lapalme, C., Davila, A. F., Pollard, W., Marinova, M., Heldmann, J., & McKay, C. P., 2016. Solar radiation and air and ground temperature relations in the cold and hyper-arid Quartermain Mountains, McMurdo Dry Valleys of Antarctica. Permafr. Periglac. Process. 27, 163-176.
41. Levy, J. S., Fountain, A. G., Dickson, J. L., Head, J. W., Okal, M., Marchant, D. R., & Watters, J., 2013. Accelerated thermokarst formation in the McMurdo Dry Valleys, Antarctica. Sci. Rep. 3, 2269.
42. MacIntyre, C., Risk, D., Lee, C.K., & Cary, S.C., 2019. Processes driving soil CO_2 temporal variability in Antarctic Dry Valleys. Geoderma 337, 871-879.
43. Mazzini, A., Lupi, M., Sciarra, A., Hammed, M., Schmidt, S.T. and Suessenberger, A., 2019. Concentric Structures and Hydrothermal Venting in the Western Desert, Egypt. Front. Earth Sci. 7, 266. doi: 10.3389/feart.2019.00266.
44. Mikucki, J. A., Auken, E., Tulaczyk, S., Virginia, R. A., Schamper, C., Sørensen, K. I., Doran P. T., Dugan H. & Foley, N., 2015. Deep groundwater and potential subsurface habitats beneath an Antarctic dry valley. Nat. Commun. 6, 6831. doi: 10.1038/ncomms7831.
45. Monaghan, A.J., Bromwich, D.H., Powers, J.G., Manning, K.W., 2005. The Climate of the McMurdo, Antarctica, Region as Represented by One Year of Forecasts from the Antarctic Mesoscale Prediction System. J. Climate 18, 1174–1189.
46. Moore, T.R., & Knowles, R., 1987. Methane and carbon dioxide evolution from subarctic fens. Can. J. Soil Sci. 67, 77-81.
47. Murrell, B., 1973. Cenozoic stratigraphy in Lower Taylor Valley, Antarctica. N. Z. J. Geol. Geophys. 16, 225-242.
48. Obryk, M.K., Doran, P.T., Fountain, A.G., Mayers, M., McKay, C.P., 2020. Climate from the McMurdo Dry Valleys, Antarctica, 1986-2017: surface air temperature trends and redefined summer season. Journal of Geophysical Research: Atmospheres, 125(13), p.e2019JD032180

564 49. Oechel, W.C., Hastings, S.J., Vourlrtis, G., Jenkins, M., Riechers, G., & Grulke, N., 1993.
565 Recent change of Arctic tundra ecosystems from a net carbon dioxide sink to a source. Nature
566 361, 520-523.
567 50. Oertel, C., Matschullat, J., Zurba, K., Zimmermann, F., & Erasmi, S., 2016. Greenhouse gas
568 emissions from soils-A review. Geochemistry 76, 327-352.
569 https://doi.org/10.1016/j.chemer.2016.04.002
570 51. Parsons, A.N., Barrett, J.E., Wall, D.H., Virginia, R.A., 2004. Soil Carbon Dioxide Flux in
571 Antarctic Dry Valley Ecosystems. Ecosystems 7, 286–295.
572 52. Risk, D., Lee, C. K., MacIntyre, C., & Cary, S. C., 2013. First year-round record of Antarctic
573 Dry Valley soil CO_2 flux. Soil Biol. Biochem. 66, 193-196.
574 53. Romanak, K.D., Bennett, P.C., Yang, C., & Hovorka, S.D., 2012. Process-based approach to
575 CO_2 leakage detection by vadose zone gas monitoring at geologic CO_2 storage sites. Geophys.
576 Res. Lett. 39.
577 54. Schuur, E. A., Bockheim, J., Canadell, J. G., Euskirchen, E., Field, C. B., Goryachkin, S. V.,
578 Hagemann S., Kuhry P., Lafleur P.M., Lee H., Mazhitova G., Nelson F.E., Rinke A.,
579 Romanovsky V.E., Shiklomanov N., Tarnocai C., Venevsky S., Vogel J.G. & Zimov, S. A.,
580 2008. Vulnerability of permafrost carbon to climate change: Implications for the global carbon
581 cycle. BioScience 58, 701-714.
582 55. Schuur, E. A., McGuire, A. D., Schädel, C., Grosse, G., Harden, J. W., Hayes, D. J., Hugelius
583 G., Koven C. D., Kuhry P., Lawrence D. M., Natali S. M., Olefeldt D., Romanovsky V. E.,
584 Schaefer K., Turetsky M. R., Treat C. C. & Vonk, J. E., 2015. Climate change and the
585 permafrost carbon feedback. Nature 520, 171-179. doi:10.1038/nature14338
586 56. Schuur, E.A.G., Vogel, J.G., Crummer, K.G., Lee, H., Sickman, J.O., Osterkamp, T.E., 2009.
587 The effect of permafrost thaw on old carbon release and net carbon exchange from tundra.
588 Nature 459, 556–559.
589 57. Sciarra, A., Mazzini, A., Inguaggiato, S., Vita, F., Lupi, M., Hadi, S., 2018. Radon and carbon
590 gas anomalies along the Watukosek Fault System and Lusi mud eruption, Indonesia. Mar. Pet.
591 Geol. 90, 77-90. https://doi.org/10.1016/j.marpetgeo.2017.09.031
592 58. Sciarra, A., Cantucci, B., Ricci, T., Tomonaga, Y., & Mazzini, A., 2019. Geochemical
593 characterization of the Nirano mud volcano, Italy. Appl. Geochem. 102, 77-87.
594 https://doi.org/10.1016/j.apgeochem.2019.01.006
595 59. Sciarra, A., Cantucci, B., Sapia, V., De Ritis, R., Ricci, T., Civico, R., Galli G., Cinti D. &
596 Coltorti, M. 2021. Geochemical and geoelectrical characterization of the Terre Calde di

Medolla (Emilia-Romagna, northern Italy) and relations with 2012 seismic sequence. J. Geochem. Explor. 221. https://doi.org/10.1016/j.gexplo.2020.106678

60. Shanhun, F. L., Almond, P. C., Clough, T. J., & Smith, C. M., 2012. Abiotic processes dominate CO_2 fluxes in Antarctic soils. Soil Biol. Biochem. 53, 99-111.
61. Shannon, G., Heyes, A., Moore, T., 1993. Carbon dioxide and methane fluxes from drained peat soils, southern Quebec. Glob. Biogeochem. Cycles 7, 247-257.
62. Shindell, D.T., Schmidt, G.A., 2004. Southern hemisphere climate response to ozone changes and greenhouse gas increase. Geophys. Res. Lett. 31, L18209.
63. Sinclair, A. J., 1991. A fundamental approach to threshold estimation in exploration geochemistry: probability plots revisited. J. Geochem. Explor. 41, 1-22.
64. Sommerfeld, R.A., Mosier, A.R., & Musselman, R.C., 1993. CO_2, CH_4 and N_2O flux through a Wyoming snowpack and implications for global budgets. Nature 361, 140-142.
65. Swanger, K.M., Marchant, D.R., 2007. Sensitivity of ice-cemented Antarctic soils to greenhouse-induced thawing: are terrestrial archives at risk? Earth Planet. Sci. Lett. 259, 347–359.
66. Swanger, K.M., Marchant, D.R., Kowalewski, D.E., Head, J.W., 2010. Viscous flow lobes in central Taylor Valley, Antarctica: origin as remnant buried glacial ice. Geomorphology 120, 174–185.
67. Turetsky, M.R., Wieder, R.K., & Vitt, D.H., 2002. Boreal peatland C fluxes under varying permafrost regimes. Soil Biol. Biochem. 34, 907-912.
68. Van Everdingen, R., 2005. Multi-language glossary of permafrost and related ground-ice terms. National Snow and Ice Data Center/World Data Center for Glaciology, Boulder, CO. http://nsidc. org/fgdc/glossary.
69. Virginia, R.A., Wall, D.H., 1999, How Soils Structure Communities in the Antarctic Dry Valleys. Bioscience 49, 973–983.

Vitt, D.H., & Chee, W.L., 1990. The relationships of vegetation to surface water chemistry and peat chemistry in fens of Alberta, Canada. Vegetatio 89, 87-106. https://doi.org/10.1007/BF00032163

70. Voigt, C., Marushchak, M. E., Mastepanov, M., Lamprecht, R. E., Christensen, T. R., Dorodnikov, M., Jackowicz-Korczyński M., Lindgren A., Lohila A., Nykänen H., Oinonen M., Oksanen T., Palonen V., Treat C.C., Martikainen P.J. & Biasi, C., 2019. Ecosystem carbon response of an Arctic peatland to simulated permafrost thaw. Glob. Change Biol. 25, 1746-1764.

71. Xue, K., Yuan, M. M., Shi, Z. J., Qin, Y., Deng, Y. E., Cheng, L., Wu L., He Z., Van Nostrand J.D., Bracho R., Natali S., Schuur E.A.G., Luo C., Konstantinidis K.T., Wang Q., Cole J.R., Tiedje J.M., Luo Y. & Zhou, J., 2016. Tundra soil carbon is vulnerable to rapid microbial decomposition under climate warming. Nat. Clim. Change 6, 595-600.
72. Zhu, R., Liu, Y., Xu, H., Huang, T., Sun, J., Ma, E., & Sun, L., 2010. Carbon dioxide and methane fluxes in the littoral zones of two lakes, east Antarctica. Atmos. Environ. 44, 304-311.

Acknowledgments

This work is part of the PNRA 2018/D3.01 SENECA project and was financially supported by CNR (PNRA 2018 n° 00253 linea D, prot.73633/2019, SENECA PROJECT: Source and origin of greenhouses gases in Antarctica). All the data were collected during the XXXV Italian expedition in Antarctica, we thank PNRA and UTA ENEA for the logistic support. SENECA is a joint project of international cooperation between Italy, New Zealand and Norway. We thank the Antarctica New Zealand for the scientific, logistical and technical support and the Scott Base personnel for hosting our research team. We acknowledge the support of the Research Council of Norway (NFR) through the HOTMUD project number 288299 and its Centres of Excellence funding scheme, project number 223272 (CEED).

Authors Contributions

L.R., A.S. and G.W. led the conceptual development of the study and designed the project. L.R., A.S., A.M., F.F., G.W., C.M., M.C.T., J.T.H.A., R.W. and V.R. data collection. A.S. and M.C.T. analysed the data. L.R., A.S., G.C. and A.M. interpreted the data. L.R., A.S. and G.C. wrote original manuscript. L.R., A.S., A.M., J.T.H.A, F.F., G.W., R.S., C.M., V.R. and S.B. drafted the paper. L.R. Principal Investigator of the SENECA project.

Competing interests

The authors declare no competing financial interests.

Supplementary materials

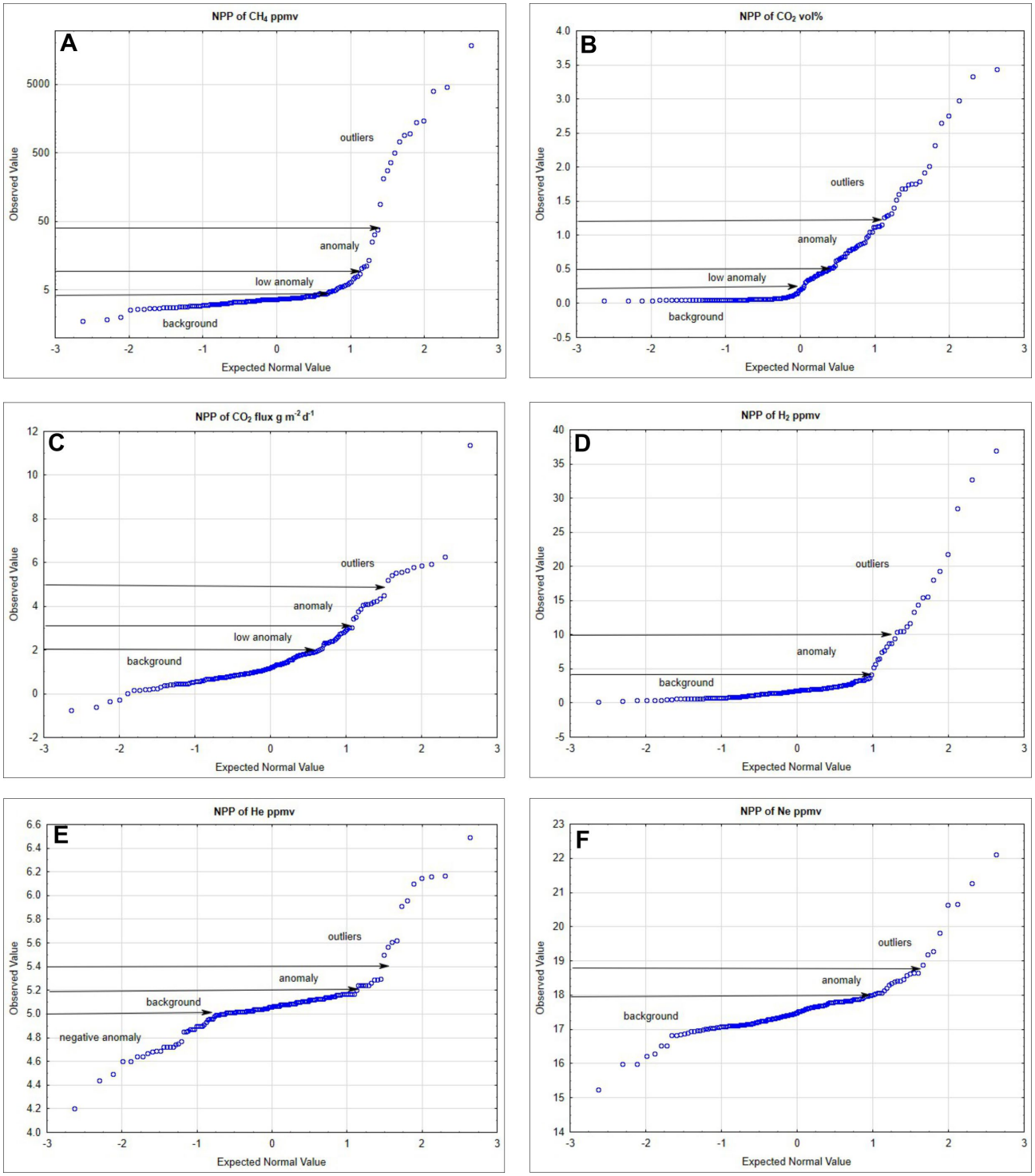

Figure S1. Normal Probability Plots of CO_2 (A), CH_4 (B), φCO_2 (C), H_2 (D), He (E), Ne (F) measurements carried out the Taylor Valley, Antarctica. The graphs also show the different populations recognized for each gas species.

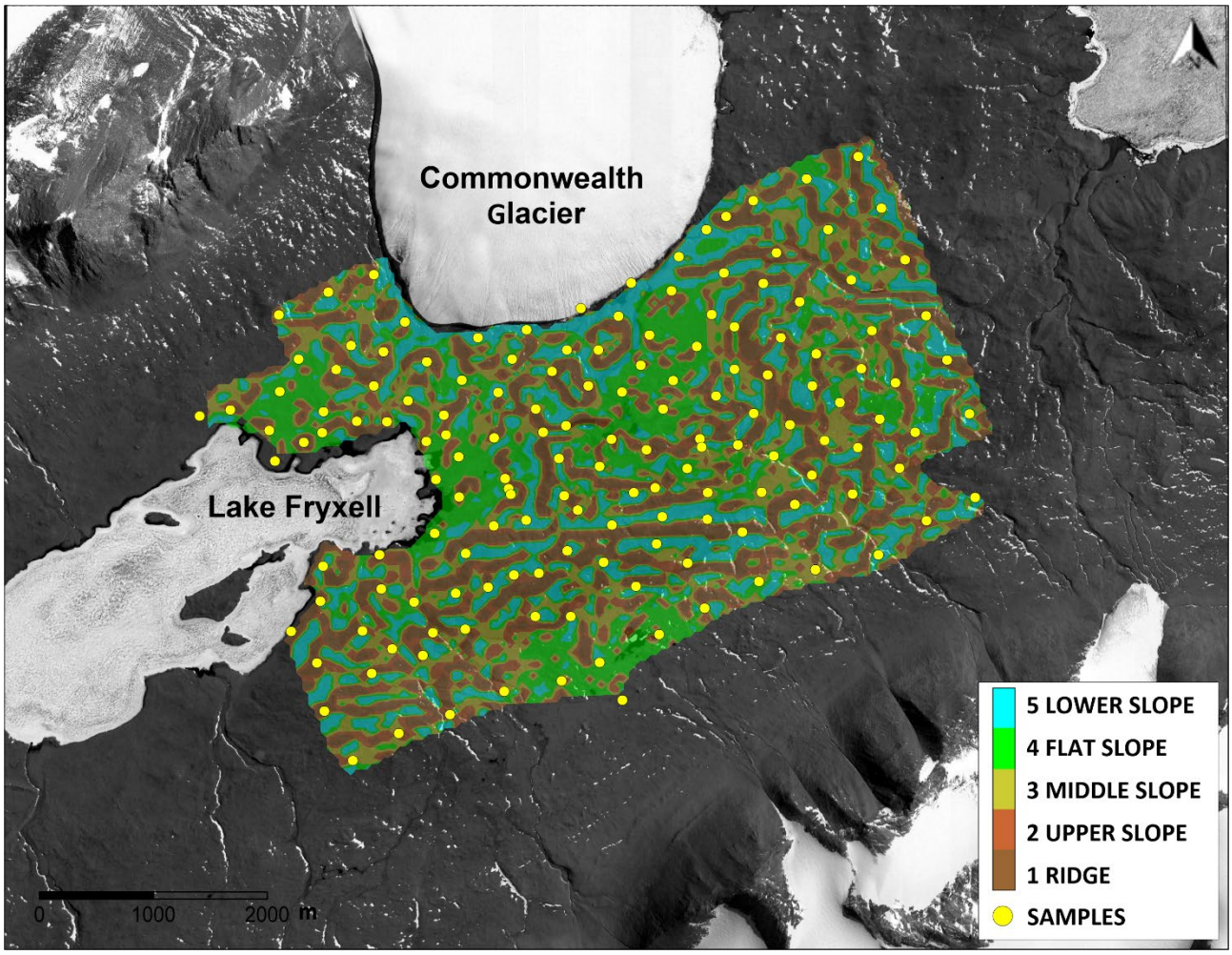

Figure S2. TPI slope position map of the study area, Taylor Valley, Antarctica. For its elaboration the high precision DEM has been used, resampled with 50m cells. The resulting map show the presence of 5 classes of slopes. Class 6 "Valley" is not present in the selected area.

Table S1. Output of φCO_2 measurements carried out at Taylor Valley, Antarctica. The total gas emission rates over the surveyed surface (21.6 km^2) have been computed following the Chiodini and Frondini (2001) approach. Background values were not included.

Population classes	average ($g\ m^{-2}d^{-1}$)
φCO_2	
2-3	2.47
3-5	3.89
>5	6.26
tons day^{-1}	**14.95**

Table S2. Comparison of gas content measured in the Lower Taylor Valley and air composition at different layers in the surficial environment. Typical average values of soil gas concentration of Ne,

675 O_2, N_2, H_2O, Ar, CO_2, He, CH_4, and H_2 in the Taylor Valley (this work), atmospheric air, atmosphere-
676 soil interface and soil gas.

	Taylor Valley (this work)	Atmospheric air	Atmosphere-soil interface	Soil gas
N_2 (vol%)	76.18	78.08	78.08	79.2
O_2 (vol%)	20.82	20.95	20.94	20.6
H_2O (%)	-	0.1 – 4	na	na
Ar (%)	-	0.93	0.93	na
CO_2 (vol%)	0.53	0.04	0.031	0.25
Ne (ppmv)	17.61	18	na	na
He (ppmv)	5.08	5.24	5.22*	na
CH_4 (ppmv)	220.3	1.9	1.4	na
H_2 (ppmv)	3.57	0.5	0.5	na

677 Modified from Rose et al. (1979); *Holland & Emerson (1990).
678
679 **Table S3**. Statistics of soil gas concentration of He, Ne, H_2, O_2, N_2, CH_4, CO_2 and φCO_2 in the 5 slope
680 classes defined by TPI slope position analysis. 1: Ridge; 2: Upper slope; 3: Middle slope; 4: Flat slope; 5:
681 Lower slope.

	TPI-Slope class	N	Mean	Median	Min	Max	SD	CV
He (ppmv)	1	12	5.10	5.06	4.77	5.61	0.20	3.89
Ne (ppmv)	1	12	17.61	17.39	17.10	19.82	0.75	4.24
H_2 (ppmv)	1	12	5.78	1.80	0.61	36.95	10.27	177.56
O_2 (vol%)	1	12	20.87	20.88	20.68	21.06	0.11	0.52
N_2 (vol%)	1	12	76.25	76.25	75.91	76.57	0.20	0.26
CH_4 (ppmv)	1	12	45.89	3.73	2.69	506.10	144.94	315.81
CO_2 (vol%)	1	12	0.28	0.08	0.05	0.80	0.31	110.97
φCO_2 (g $m^{-2}d^{-1}$)	1	12	1.36	0.85	-0.61	4.35	1.50	110.52
He (ppmv)	2	11	5.01	5.02	4.68	5.57	0.27	5.32
Ne (ppmv)	2	11	17.86	17.66	15.99	20.66	1.24	6.96
H_2 (ppmv)	2	11	4.92	1.95	0.46	19.35	6.57	133.56
O_2 (vol%)	2	11	20.80	20.81	20.62	20.94	0.12	0.60
N_2 (vol%)	2	11	76.17	76.23	75.22	76.87	0.52	0.68
CH_4 (ppmv)	2	11	3.64	3.60	2.61	5.49	0.76	20.85
CO_2 (vol%)	2	11	0.34	0.06	0.05	1.74	0.52	153.15
φCO_2 (g $m^{-2}d^{-1}$)	2	11	1.83	1.17	0.42	5.77	1.89	103.15
He (ppmv)	3	105	5.10	5.07	4.44	6.49	0.31	6.17
Ne (ppmv)	3	105	17.54	17.45	15.23	21.26	0.71	4.04
H_2 (ppmv)	3	105	3.28	1.79	0.15	28.50	4.63	141.34
O_2 (vol%)	3	105	20.82	20.88	19.52	21.05	0.23	1.09
N_2 (vol%)	3	105	76.13	76.23	74.23	77.11	0.57	0.74
CH_4 (ppmv)	3	105	283.93	3.69	1.75	18446.56	1858.97	654.73
CO_2 (vol%)	3	105	0.58	0.20	0.04	3.44	0.78	134.06
φCO_2 (g $m^{-2}d^{-1}$)	3	106	1.66	1.15	-0.74	6.25	1.44	86.70
He (ppmv)	4	17	4.98	5.07	4.20	5.29	0.29	5.90

Ne (ppmv)	4	17	17.47	17.63	16.29	18.66	0.61	3.50
H_2 (ppmv)	4	17	3.59	1.67	0.28	32.71	7.57	210.62
O_2 (vol%)	4	17	20.82	20.89	20.42	21.09	0.18	0.86
N_2 (vol%)	4	17	76.46	76.46	75.72	77.19	0.41	0.54
CH_4 (ppmv)	4	17	237.96	3.67	2.81	3977.37	963.63	404.95
CO_2 (vol%)	4	17	0.42	0.52	0.05	0.90	0.35	82.60
φCO_2 (g $m^{-2}d^{-1}$)	4	18	2.17	1.66	-0.34	11.36	2.55	117.90
He (ppmv)	5	12	5.01	5.04	4.72	5.13	0.13	2.53
Ne (ppmv)	5	12	17.91	17.70	17.08	19.28	0.76	4.25
H_2 (ppmv)	5	12	3.10	2.34	0.67	8.80	2.80	90.31
O_2 (vol%)	5	12	20.79	20.84	20.52	20.95	0.15	0.72
N_2 (vol%)	5	12	76.06	76.08	75.29	76.91	0.49	0.65
CH_4 (ppmv)	5	12	3.83	3.58	3.12	6.12	0.99	25.77
CO_2 (vol%)	5	12	0.69	0.45	0.06	1.68	0.54	78.81
φCO_2 (g $m^{-2}d^{-1}$)	5	12	1.73	1.57	0.38	5.53	1.68	96.99

N: number of observations; SD: standard deviation; CV: coefficient of variation.

Table S4. Statistics of soil gas concentration of He, Ne, H_2, O_2, N_2, CH_4, CO_2 and φCO_2 in the Lower Taylor Valley wetlands.

	N	Mean	Median	Min	Max	LQ	UQ	P10%	P90%	SD	SK
He (ppmv)	16	5.00	5.06	4.64	5.15	5.0	5.09	4.68	5.14	0.15	-1.66
Ne (ppmv)	16	17.36	17.31	16.84	17.78	17.15	17.64	16.85	17.70	0.30	-0.31
H_2 (ppmv)	16	5.54	1.59	0.46	36.95	0.93	2.81	0.51	19.35	9.87	2.62
O_2 (vol%)	16	20.8	20.9	20.6	21.0	20.8	20.9	20.6	21.0	0.1	-0.9
N_2 (vol%)	16	76.3	76.3	75.7	77.1	76.0	76.6	75.8	76.8	0.4	0.4
CH_4 (ppmv)	16	3.6	3.5	2.0	6	3.0	4.1	2.8	4.9	1	0.6
CO_2 (vol%)	16	0.29	0.09	0.05	1.05	0.06	0.54	0.05	0.69	0.32	1.22
φCO_2 (g $m^{-2}d^{-1}$)	16	1.27	0.94	-0.26	4.11	0.67	1.84	0.32	2.73	1.08	1.30

N: number of observations; LQ: lower quartile; UQ: upper quartile; P10%: percentile 10%; P90%: percentile 90%; SD: standard deviation; SK: skewness.

References

Holland, P.W., & Emerson, D.E., 1990. The global helium-4 content of near-surface atmospheric air. In Geochemistry of gaseous elements and compounds, pp. 97-109.

Rose A.W., Hawkes H.W., Webb J.S., 1979. Geochemistry in mineral exploration. Second Edition, Academic Press, London, 657 pp.